# Comparative assessment of the chronic effects of five nano-perovskite to *Daphnia magna*: a structure based toxicity mechanism

Tingting Zhou, Wenhong Fan*, Yingying Liu, and Xiangrui Wang

## Supplementary Information

Number of supplementary information pages: 11

Number of Tables: 3

Number of Figures: 4

## Materials and Methods

### Synthesize of PNMs

$LaFeO_3$:

$LaFeO_3$ were prepared by hydrothermal method according to Yang, W., et al. [1]. Briefly, certain amount of $La(NO_3)_3 \bullet 6H_2O$ and ferric acetylacetonate were weighed precisely according to the atomic ratio of the target product and dissolved in benzoic acid at 80°C. Transparent solution were transferred to Teflon-lined autoclave, and was hydrothermally processed at 200 ° C for 24h. Obtained turbid liquid was washed by D.I. water and ethanol through centrifugation and then dried at 80 ° C for 12 h. The precursor was calcined at 500 ° C for 6 h.

$YFeO_3$:

Hydrothermal method was also used in $YFeO_3$ synthesis[2]. $Fe(NO_3)_3 \bullet 9H_2O$ and $Y(NO_3) \bullet 6H_2O$ were dissolved in D.I. water and then a certain amount of polyvinyl alcohol solution were added under magnetic stirring. After that, urea was added to the mixed solution, urea concentration was selected to be two times of total number of moles of nitrate ions. After

stirring for an hour in water bath at 60 °C, the solution were transferred to Teflon-lined autoclave. The autoclave was heated at 200 °C for 6 h. The product is washed with distilled water and alcohol to remove any by-product, dried at 100 °C and then calcined to form the perovskite phase of the oxide powders at 800 °C for 2h.

$BiFeO_3$:

$BiFeO_3$ were prepared by sol-gel method according to literature with slight modifications[3]. $Bi(NO_3)$ $\bullet 5H_2O$ and were first dissolved in nitric acid, than the obtained solution and $Fe(NO_3)_3 \bullet 9H_2O$ were dissolved in 30ml 2-methoxyethanol. The solution was stirred to transparent and corresponding amount of malonic acid and ethylene glycol was added. The mixed solution was maintained at 70 °C in a water bath for gelation. The gel was dried at 100 °C for 24 h. The precursor was calcined at 500 °C for 1 h.

$LaMnO_3$:

$LaMnO_3$ were prepared by sol-gel method according to literature with slight modifications[4]. $La(NO_3)_3 \bullet 6H_2O$ and equivalent of $Mn(CH_3COO)_2 \bullet H_2O$ were dissolved in D.I. water, citric acid were added slowly under magnetic stirring. The solutions were evaporated at 80 °C in water bath for 3h to form sol. The sol were dried at 110 °C for 8h and completely powdered and calcined at 650 °C for 9 h.

$LaCoO_3$:

Coprecipitation method was used according to Chandradass, J., et al.[5]: stoichiometric amounts of $La(NO_3)_3 \bullet 6H_2O$ and $Co(NO_3)_2 \cdot 6H_2O$ were dissolved in 80ml ethanol, then ammonia water were added dropwise under stirring to form $La(OH)_3$ and $Co(OH)_2$ and the final pH was 9. The suspension were stirred for two more hours. The precipitate were washed with ethanol for many times and dried at 80 °C for 48h and calcined at muffle at 600 °C for 2h.

**Characterization of materials**

X-Ray diffraction (XRD) was done recorded using a Bruker D8 Advance diffractometer equipped with Cu-K$\alpha$ source. The data were collected by using step scanning at $2\theta$ =10-90°

with step size of 0.058. The structural and microstructural parameters (the phase compositions, structure, lattice parameters) were extracted using Rietveld refinement by applying the Topas program. The Rietveld's method has given a reasonable fit of the diffraction profiles (Rwp<15%, $\chi$ <2). Nitrogen adsorption-desorption isotherms (Micromeritics ASAP2020, America) were measured for BET surface area calculation. X-ray photoelectron spectroscopy (XPS, ThermoFisher K-Alpha, USA) was used to analysis the elements on PNMs surface, the binding energy were calibrated by C 1s at 284.6 eV. TEM (TEM; Hitachi 7500) were used to evaluate size distribution.

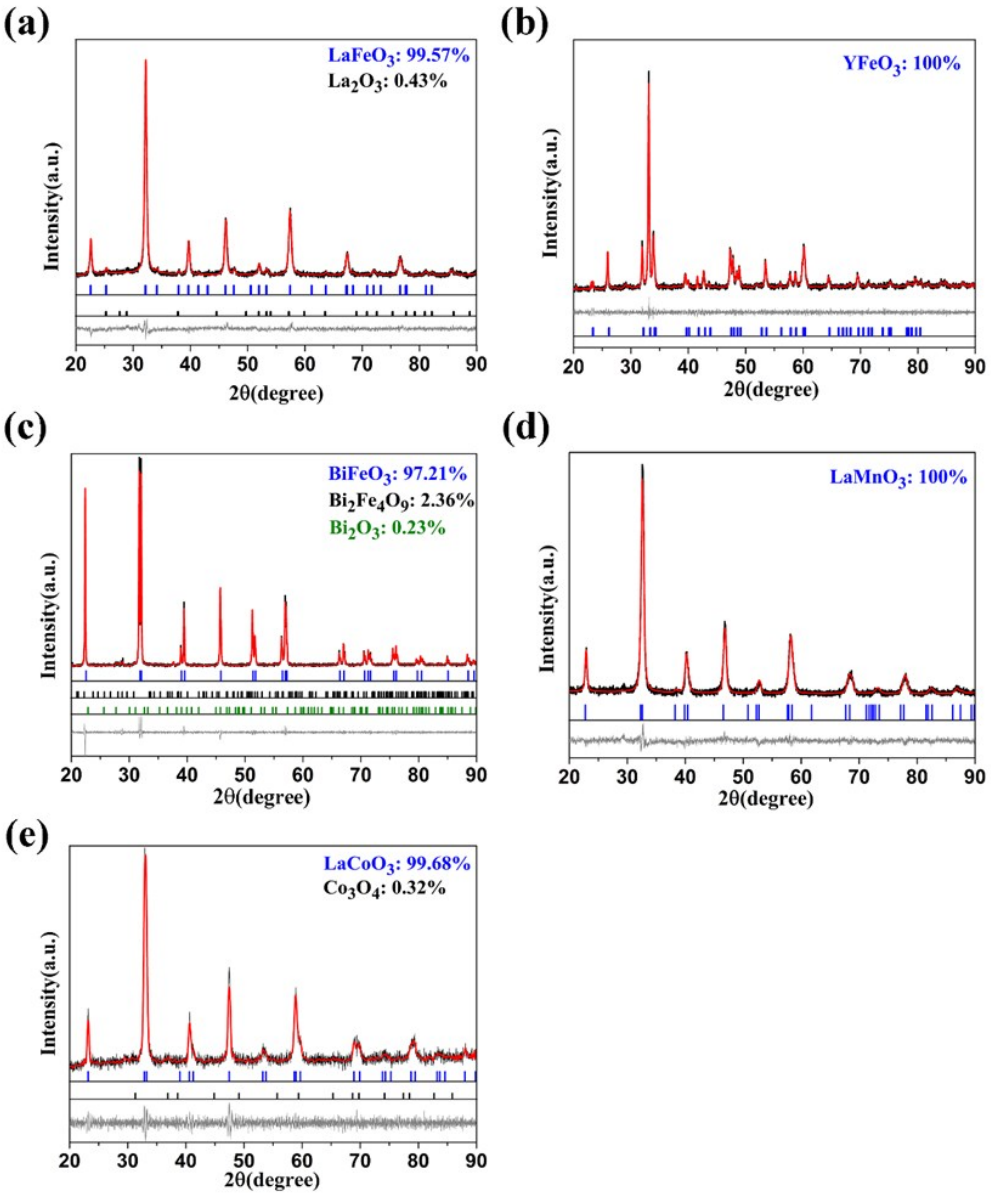

**Figure S1.** XRD patterns of five synthesized PNMs: (a) $LaFeO_3$ (b) $YFeO_3$ (c) $BiFeO_3$ (d) $LaMnO_3$ (e) $LaCoO_3$

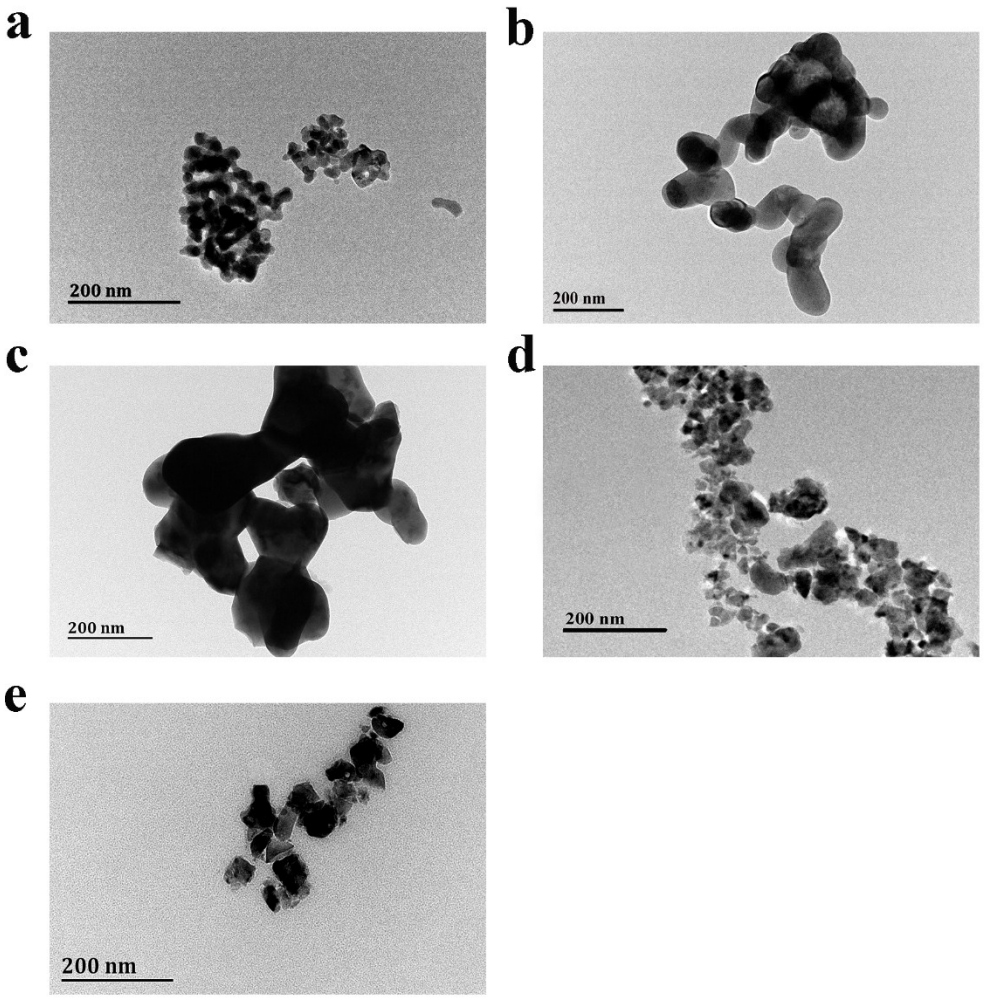


**Figure S2.** Transmission electron micrograph images of PNMs: (a) $LaFeO_3$ (b) $YFeO_3$ (c) $BiFeO_3$ (d) $LaMnO_3$ (e) $LaCoO_3$

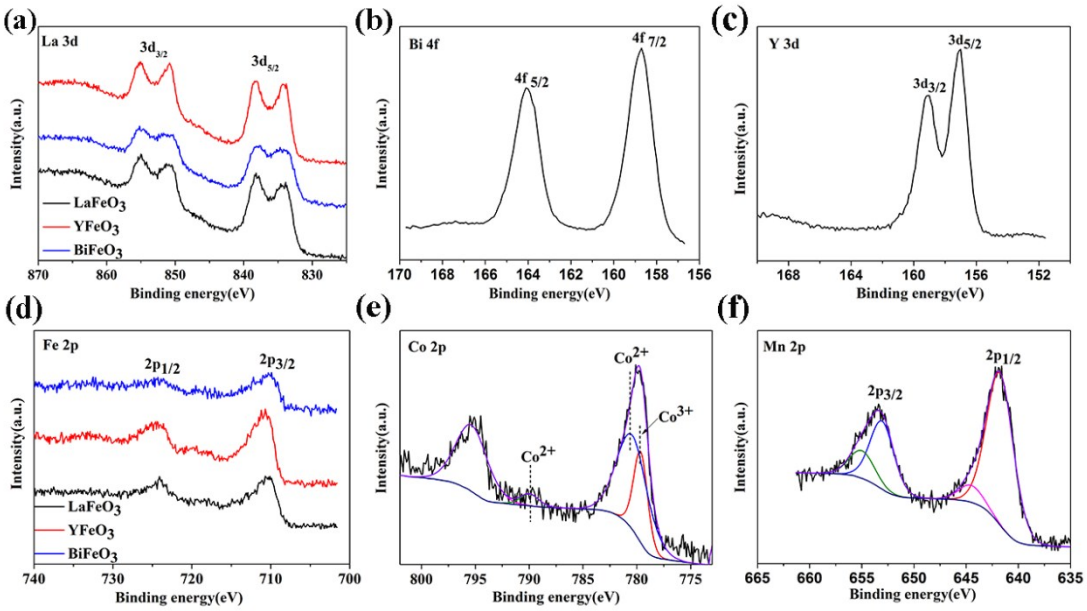


**Figure S3.** XPS spectra of elements of five synthesized PNMs: (a) La 3d (b) Bi 4f (c) Y 3d (d) Fe 2p (e) Co 2p (f) Mn 2p

Analysis of the photoelectron spectrum La 3d (**Figure S3a**) reveals the presence of intense lines of the shake-up satellite (binding energy = 838.0 and 856 eV) and the spin-orbit splitting between peaks La $3d_{5/2}$ and La$3d_{3/2}$ equal to 16.8 eV that leads us to conclude about predominant state $La^{3+}$ in the complex oxide[6]. The binding energy of Bi (**Figure S3b**) located at 164.1 and 158.7 eV correspond to the Bi $4f_{5/2}$ and Bi $4f_{7/2}$ orbitals in the trivalent oxidation state [7]. Characteristic binding energy values of 157.1 eV for Y 3d5/2 and 159.0 eV for Y 3d3/2 (**Figure S3c**)prove a trivalent oxidation state for yttrium[8]. In the XPS spectra of Fe in Fe-contained PNMs (**Figure S3d**), the Fe $2p_{3/2}$ peaks are located in 710.7, 710.7, 710.4eV, respectively. They all are close to the values recorded for $Fe^{3+}$ (around 710.5–710.8 for Fe 2p3/2), revealed shape characteristic of the $Fe^{3+}$ state[6, 9]. In the XPS spectra of Fe (II), the satellite peak of Fe $2p_{3/2}$ is located 5-6eV higher than the main Fe $2p_{3/2}$ peak. The satellite peaks of Fe $2p_{3/2}$ were much closer to Fe $2p_{1/2}$ peaks in our samples, indicating there are no

$Fe^{2+}$ existence in Fe-contained perovskites used this study. The XPS spectra of Co 2p level is shown in Figure S3e. The Co 2p XPS spectra exhibited two main peaks corresponding to the $2p_{3/2}$ and $2p_{1/2}$ levels and one shake-up satellite peak centered at ca. 790.0 eV. The asymmetric peak of Co $2p_{3/2}$ could be resolved into two components, the peak at lower BE was attributed to $Co^{3+}$ in perovskite[10], the peak located at higher BE was close to the peak position of CoO[11]. The results suggest that there were $Co^{2+}$ and $Co^{3+}$ in the $LaCoO_3$ nanoparticle. The $Mn2p_{3/2}$ profile (**Figure S3f**) changes to a value at 641.9 eV that is consistent with the expected BE for $Mn^{3+}$ species[12]. The manganese species corresponding to the BE at 643 eV would be Mn4+ species[13, 14]. In the case of manganese, the absence of a satellite peak at +5 eV from the Mn $2p_{3/2}$ indicates that no $Mn^{2+}$ is present[15].

**Table S1.** Selected properties of five synthesized PNMs: (a) $LaFeO_3$ (b) $YFeO_3$ (c) $BiFeO_3$ (d) $LaMnO_3$ (e) $LaCoO_3$; hydrodynamic diameter and zeta-potential of raw-PNM and GA-PNM suspension.

| | Tolerance factor | Crystal structure | BET surface area ($m^2/g$) | Valance state | | O□□/ O (%) | Particle size (nm) | Zeta potential (mV) | |
|---|---|---|---|---|---|---|---|---|---|
| | | | | | | | | Raw-PNMs | GA- PNMs |
| $LaFeO_3$ | 0.95 | Tetragonal (Pnma) | 41.96 | La<br>Fe | III<br>III | 57 | 31.5±11.9 | -4.94 ± 0.76 | -12.8 ± 1.16 |
| $YFeO_3$ | 0.80 | Tetragonal (Pnma) | 7.13 | Y<br>Fe | III<br>III | 41 | 122±38.5 | -8.29 ± 0.26 | -14.4 ± 1.34 |
| $BiFeO_3$ | 0.96 | Hexagonal (R3cH) | 0.933 | Bi<br>Fe | III<br>III | 37 | 178±64.3 | -5.53 ± 0.52 | -12.2 ± 0.85 |
| $LaMnO_3$ | 0.95 | Hexagonal (R3cH) | 11.53 | La<br>Mn | III<br>III, IV | 43 | 32.3±14 | -7.58 ± 1.78 | -12.4 ± 3.72 |
| $LaCoO_3$ | 0.97 | Cubic (Pm3m) | 8.38 | La<br>Co | III<br>II, III | 62 | 49±13.9 | -6.19 ± 1.81 | -13.7 ± 0.72 |

**Table S2.** Time-weighted average concentration of five PNMs in six nominal concentrations.

| Nominal concentration (mg/L) | | 0.5 | 1 | 5 | 10 | 25 | 50 |
|---|---|---|---|---|---|---|---|
| Actual concentration (mg/L) | $LaFeO_3$ | 0.2 | 0.4 | 1.4 | 2.4 | 9.7 | 21.2 |
| | $YFeO_3$ | 0.2 | 0.2 | 0.8 | 1.7 | 4.1 | 11.9 |
| | $BiFeO_3$ | 0.1 | 0.1 | 0.2 | 0.4 | 0.8 | 1.5 |
| | $LaMnO_3$ | 0.1 | 0.2 | 1.4 | 1.1 | 2.7 | 7. 5 |
| | $LaCoO_3$ | 0.2 | 0.3 | 0.8 | 1.4 | 13 | 5.4 |

Time-weighted average concentration(TWA) were calculated using concentrations measured in time(0, 6, 24, 48h) according to the following equation[16].

$$TWA = \frac{\sum_{n=1}^{N} (\Delta t_n \frac{C_{n-1} + C_n}{2})}{\sum_{n=1}^{N} (\Delta t_n)}$$

Where TWA = Time weighted average concentration (mg/L); $\Delta$t = time interval between measurements (h); n = time interval number; N = total number of time intervals; c = concentration measured at end of time interval (mg /L).

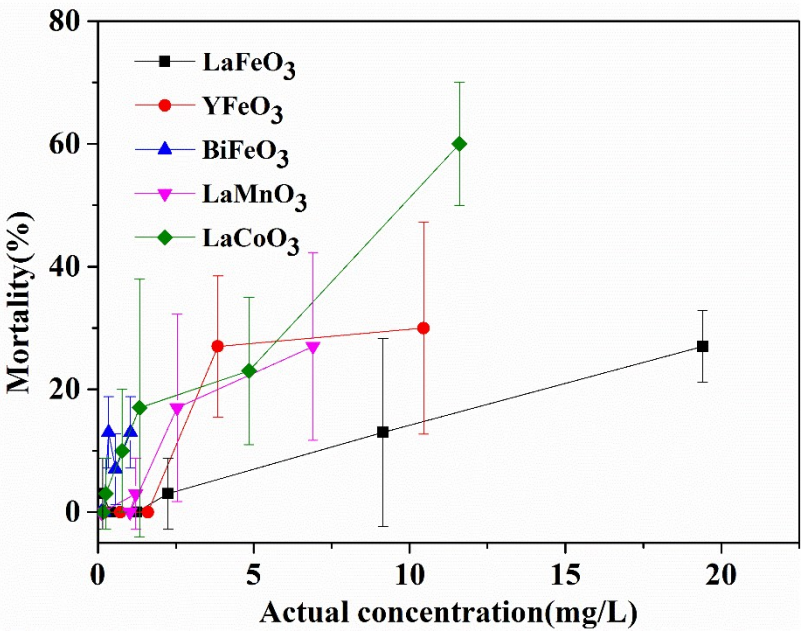


**Figure S4.** Effect of PNMs on acute daphnid mortality. Values are means ± SD (n = 3).

**Table S3.** Data of D. magna collected by 21-day chronic assay during exposure to five PNMs suspensions in the absence and presence of GA. Molts per female, body length, time to first brood, broods per female, average neonates female are expressed as the mean ± standard deviation. * indicate significant differences between the treatment and control groups ($p < 0.05$), # indicate significant differences between the absence and presence of GA for each PNM treatment ($p < 0.05$).

| | | Mortality (%) | Molts per female (number) | Body length(nm) | | | Broods per female (number) | Average neonates per female (number) |
|---|---|---|---|---|---|---|---|---|
| | | | | 7d | 14d | 21d | | |
| | SM7 | 5 | 9.3± 0.6 | 2.05±0.08 | 2.54± 0.09 | 3.00±0.10 | 3.9±0.9 | 22.4±4.2 |
| | GA | 5 | 9.1± 0.8 | 2.05±0.07 | 2.52± 0.10 | 2.99±0.12 | 4.2±0.5 | 21.5±5.4 |
| Raw | $LaFeO_3$ | 15 | 9.4± 0.7 | 2.12±0.10* | 2.54±0.13 | 2.97±0.15 | 3.6±0.5 | 19.4±7.0 |
| | $YFeO_3$ | 15 | 8.3± 0.5* | 2.09 ± 0.11 | 2.58±0.09 | 2.95±0.08 | 3.7±0.7 | 19.6±4.1 |
| | $BiFeO_3$ | 0 | 9.3± 0.5 | 2.07 ± 0.10 | 2.45±0.09* | 2.91±0.13* | 3.6±0.5 | 19.9±4.8 |
| | $LaMnO_3$ | 15 | 9.7± 1.0 | 2.07± 0.09 | 2.54±0.10 | 2.94±0.13 | 3.9±0.6 | 23.3±6.7 |
| | $LaCoO_3$ | 100 | -- | 1.61± 0.11* | -- | -- | -- | -- |
| GA- | $LaFeO_3$ | 50 | 9.7± 0.5 | 2.08±0.08 | 2.56±0.14 | 2.99±0.07 | 3.8±0.4 | 19.4±2.6 |
| | $YFeO_3$ | 5 | 9.2± 0.8# | 1.94±0.12*, # | 2.61±0.12 | 3.00±0.09 | 3.6±0.7 | 19.2±3.7* |
| | $BiFeO_3$ | 30 | 9.2±0.6 | 2.09±0.11 | 2.55±0.08# | 2.82±0.08*,# | 2.4±0.5*, # | 10.5±3.1*,# |
| | $LaMnO_3$ | 30 | 9.1±0.8 | 2.05±0.10 | 2.60±0.09 | 3.00±0.08 | 3.6±0.6 | 17.4±3.0*,# |
| | $LaCoO_3$ | 95 | | 1.77±0.11*, # | 2.06±0.05* | | | |

## References


1. W. Yang, R. Zhang, B. Chen, N. Bion, D. Duprez, L. Hou, H. Zhang and S. Royer, *Chemical Communications*, 2013, **49**, 4923-4925.
2. T. Peisong, S. He, C. Haifeng and C. Feng, *Current Nanoscience*, 2012, **8**, 64-67.
3. S. V. Vijayasundaram, G. Suresh and R. Kanagadurai, *Appl. Phys. A*, 2015, **121**, 681-688.
4. T. Sanaeishoar, H. Tavakkoli and F. Mohave, *Applied Catalysis A: General*, 2014, **470**, 56-62.
5. J. Chandradass, H. Kim and F. W. Y. Momade, *Advanced Powder Technology*, 2014, **25**, 1834-1838.
6. O. P. Taran, A. B. Ayusheev, O. L. Ogorodnikova, I. P. Prosvirin, L. A. Isupova and V. N. Parmon, *Applied Catalysis B Environmental*, 2016, **180**, 86-93.
7. Navjot, A. Tovstolytkin and G. S. Lotey, *Catalysis Letters*, 2017, **147**, 1640-1645.
8. L. Wu, J. C. Yu, L. Zhang, X. Wang and S. Li, *Journal of Solid State Chemistry*, 2004, **177**, 3666-3674.
9. M. M. Natile, F. Poletto, A. Galenda, A. Glisenti, T. Montini, L. D. Rogatis and P. Fornasiero, *Chemistry of Materials*, 2008, **20**, 2314-2327.
10. H. He, H. X. Dai and C. T. Au, *Applied Catalysis B: Environmental*, 2001, **33**, 65-80.
11. W. Hai, Y. Zhu, R. Tan and W. Yao, *Catalysis Letters*, 2002, **82**, 199-204.
12. T.-K. Tseng, H. Chu and H.-H. Hsu, *Environmental Science & Technology*, 2003, **37**, 171-176.
13. G. Qi and R. T. Yang, *The Journal of Physical Chemistry B*, 2004, **108**, 15738-15747.
14. F. Wang, H. Dai, J. Deng, G. Bai, K. Ji and Y. Liu, *Environmental Science & Technology*, 2012, **46**, 4034-4041.
15. B. Kucharczyk and W. Tylus, *Applied Catalysis A General*, 2008, **335**, 28-36.
16. Y. Zhai, E. R. Hunting, M. Wouterse, P. Wjgm and M. G. Vijver, *Ecotoxicology & Environmental Safety*, 2017, **145**, 349-358.